Received July 1, 2015, accepted August 11, 2015, date of publication August 26, 2015, date of current version September 11, 2015.

Digital Object Identifier 10.1109/ACCESS.2015.2473169

Friendly Spectrally Shaped Radar Waveform With Legacy Communication Systems for Shared Access and Spectrum Management

RIC A. ROMERO, (Senior Member, IEEE), AND KEVIN D. SHEPHERD
Department of Electrical and Computer Engineering, Naval Postgraduate School, Monterey, CA 93943, USA
Corresponding author: R. A. Romero (rnromero@nps.edu)

ABSTRACT In this paper, we investigate a friendly spectrally shaped radar waveform design that can be used in a spectral band being utilized by one or more communication systems. We specifically consider legacy communication systems as opposed to cooperative communication systems to address the ever present problem of legacy technologies. This radar waveform is able to share the spectrum with the existing communication systems such that its detection performance is not compromised while trying to help the legacy systems maintain their own symbol error rates (SERs). We show with various scenarios that the spectrally shaped radar waveform outperforms the traditional wideband pulse waveform in terms of detection performance with the communication signals acting as interference to the radar. Moreover, SERs of the legacy systems employing quaternary phase-shift keying modulation in the presence of the shaped radar waveform (acting as interference) outperform SERs of systems under traditional radar pulse interference. These SERs are very close to theoretical noise-only SERs.

INDEX TERMS Friendly waveform design, spectrally-shaped waveform, spectrum sharing, electronic warfare, spectrum management, legacy communication systems.

I. INTRODUCTION

The potential interference of radars to radio or communication systems operating even in separated bands has been known for a long time [1]. It continues to be a problem today despite the fact that the radar and radio may be separated by narrow guard bands. This is because a high-power radar may spill enough power into the radio band to wipe out voice or data link functions. In fact it is a problem that is intimately known to one of the authors [2] who professionally experienced disrupted radio functions while in operations when a radar was turned on (which eventually inspired the research work herein). Some may think of this problem as a spectral crowding issue between ''friendly'' users in electronic warfare (EW) (let alone on top of the non-friendly users). Traditional solutions call for the systems to be very widely separated in the frequency domain such that systems do not interfere with one another.

Unfortunately for legacy systems (radar, radio, and otherwise), the explosion of cellular, mobile, broadband communications, and data streaming systems have placed spectral demands on traditional high-frequency bandwidth holders such as legacy radars (commercial or military) where traditional solutions are no longer feasible. In the U.S., studies have been made proposing to release some allocated legacy radar spectral bands to emerging mobile communication systems for economic reasons as well as efficient use of the electromagnetic (EM) spectrum as a resource [3]–[5]. As such various schemes such as spectral sensing, dynamic spectrum access, and non-traditional waveforms may be used by either radar or radio for the purposes of shared access and spectrum management. For example, [6] discusses opportunistic spectral sharing between radar and communication systems while [7] and [8] assess and propose cooperative spectral sensing for co-existence of a rotating radar and cellular systems. Another paper [9] illustrates that by exploring the spatial and temporal opportunities in the radar spectrum, a substantial increase on the throughput of a communications system is possible. The paper in [10] assesses the impact of secondary multiple users in radar bands using dynamic spectrum access (DAS) when spectrum sharing is performed in a totally opportunistic manner. Others have focused on radar waveform design that may be conducive to spectrum sharing. The paper in [11] proposes a system that uses orthogonal frequency division modulation (OFDM) for joint radar-radio operations. The work in [12] considers the radar ambiguity function of

OFDM signals while [13] investigates the frequency agility of OFDM signal as a radar waveform. In [14], a generalized multicarrier radar signal model is proposed that can be used to implement OFDM radar signal.

Going back to the EW perspective, it appears that the military establishment is starting to accommodate the notion of sharing allocated legacy radar bands to emerging communication systems. In [15], it is understood that the radio frequency (RF) spectrum is becoming a hotly contested resource and the U.S. Department of Defense (DoD) places a call to action to ensure reliable access to the electromagnetic spectrum for now and the future. Indeed, several organizations form the Joint Electromagnetic Spectrum Management Operations (JEMSO) to study and plan on how spectral sharing can be effectively managed [16]. Moreover, if the allocated radar bands are to be shared, then the converse is also possible, i.e., that the commercial bands may also be fair game to the newer but frequency-agile radars. The implication is that the modern battlefield grows more and more crowded with RF transmitters [17]. In other words, it has become increasingly apparent that newer systems to be fielded in the future are going to have to account for the spectral crowding problem and attempt to help manage the overall spectral environment. Thus in the battlefield (with numerous transmitters and jammers present) newer systems have to use the same portion of the spectrum that is assigned to friendly legacy systems. As mentioned, in practice total disruption to friendly radio systems is encountered when a high-powered radar system is turned on. While the OFDM-based waveforms in [11]–[13] and an information-based waveform [18] will undoubtedly prove useful in the near future, the assumption is that both or all systems are to be cooperative. Presently, legacy non-cooperative radios still exist, are still very useful in operations, and thus won't go away just yet. Thus, we need novel frequency-agile radar systems that can stay or even leave their own allocated bands and can spectrally maneuver to the legacy radio band! They should perform as designed (i.e. detect targets) in the presence of the legacy communication signals. More importantly, they should not be disruptive to those same communication signals. However, most papers concentrate on the frequency sharing implications rather than the final performance parameters that are important to radar and radio systems, i.e. detection performance P_d for radars and symbol error rate (SER) or bit error rate (BER) for radios. Very few papers deal with actual system performances of cooperative systems which are trying to share or occupy the same available spectrum. However, one paper investigates a simple setup where one radar coexists with one communication system and considers the effect on the radar's detection performance as their relative distance is varied [19].

So far as mentioned most contributions in this area concentrate on: a) cooperative systems, b) communication systems effect on operating in the radar legacy band, c) use of multicarrier-based or OFDM-based radar waveforms, and d) frequency allocation or access protocols. Our work clearly deviates from the above by considering instead: a) frequency-agile radar operating in legacy communication systems recognizing that legacy systems are still operational and that they still need to be supported, b) both radar-to-radio and radio-to-radar effects in terms of performances (radar's P_d and radio's SER), c) the use of a signal-to-interference-plus-noise SINR-based spectrally-shaped radar waveform, and d) spectral shaping of this friendly waveform as opposed to OFDM's multicarrier nature. The contributions are specified as follows. First, we consider the design of the spectrally-friendly waveform (for point targets but easily applied to extended targets) such that it mitigates the interference effects of active legacy communication systems and vice versa. Moreover, we look at the frequency implications of the spectrally-shaped radar waveform design considering that the legacy communication bandwidths are static in the frequency domain (i.e. legacy radio does not have the capability to sense radar interference or not able to maneuver when interfered upon). Furthermore, we report the detection performance P_d of the 'shaped' radar waveform and compare that to a traditional wideband pulsed waveform in the presence of 'friendly' communication systems. The term 'friendly' here clearly refers to legacy systems that are not adversaries realizing that these legacy systems are not so friendly after all (because they can also cause interference!). We also consider the converse by reporting the SER improvements of legacy communication systems with the use of the shaped radar waveform over traditional wideband radar pulse (when the radar interferes with the radio systems). It is very well known that P_d in radar is dependent on signal-to-noise ratio (SNR) or signal-to-interference-and-noise ratio (SINR). Since our goal is to report P_d for the spectrally-shaped radar waveform, we use a method for pulse shaping based on maximization of both SNR or SINR [20]–[22] which lead to ''waterfilling'' designs. Our preliminary work on this subject is reported in [23]. A good overview on spectrum sharing between radars and radios is found in [24]. Other interesting radar waveform designs with potential to be used for spectrum sharing are discussed in [25]–[27]. Other works concerning intra-pulse radar-embedded communications are found in [28] and [29]. Time-bandwidth product consideration for MIMO radar waveform design is covered in [30].

This paper is organized as follows. In Section II, we show a method for designing a waveform (for a point target which can be easily applied to an extended target) in the presence of a legacy communication signal/s in the radar's received spectrum that is based of SNR (or SINR) maximization. In Section III, we discuss the receiver for the spectrally 'shaped' radar waveform, the improved detection performance of the radar receiver (due to that waveform despite the legacy communication signal interference) as compared to a traditional wideband pulsed radar signal, and the performance impact to a communication system in terms of percentage of correct symbol detection and its more popular complement: the SER. In Section IV we consider radar detection performance P_d and SER performance when there is a

single legacy communication system operating at the same time as the radar. In Section V we consider radar detection performance and SER performances when there are multiple legacy communication systems. Finally in Section VI we present our conclusions.

II. "FRIENDLY" RADAR WAVEFORM FOR LEGACY RADIO

A. OPTIMAL RADAR SPECTRAL SHAPE FOR LEGACY COMMUNICATIONS

The goal of the SNR-based waveform design is to create a waveform (with a spectral shape) that does not interfere with friendly communications and also minimizes the 'not-so-friendly' interference effect of the communication signals on radar's detection performance. Of course, the degradation of the radar's detection performance depends on the radar SINR. Let $q(t)$ be the continuous time-domain representation of a friendly communications signal and $n(t)$ represents the additive white Gaussian noise (AWGN) out of the radar receiver. We assume that unlike the radar's signal which may be pulsed or continuous-wave (CW), the communications signal is continuous (at least during radar reception). As such prior to transmission of the radar waveform, the received signal (or interference) is given by

$$y(t) = q(t) + n(t). \tag{1}$$

It is intuitive and well known that in order to avoid a frequency band that is being utilized (here by a legacy communication system whose effect on the radar is not so friendly as evidenced by (1)), a system simply has to avoid that spectral band. Due to the communication spectral sidelobes, the question becomes how much of the spectrum is to be avoided for the benefit of the legacy system while designing the radar waveform. Clearly, the loss of that band may translate to range resolution loss for the radar waveform if that loss of band is not offset by maintaining the radar bandwidth. Of course, various techniques such as increasing the bandwidth via waveform design involving pulse compression maybe employed. Waveform design to increase effective bandwidth or improve range resolution is well known and won't be covered here. It is enough to know that it may be employed if desired. Going back to avoiding the communication band, the radar waveform designer can simply choose not to utilize the band corresponding to the mainlobe (null-to-null) of the communication signal (thereby interfering all the other sidelobes) or he may choose not to utilize the communications' 95 percent bandwidth and so on so forth. But this is simply too arbitrary. In other words, we need a waveform that efficiently uses of the spectrum while lessening the effect to the communication signals. In other words, we desire to maximize the radar SINR while meeting the transmit energy constraint. In order to find an effective transmit signal design, we use the method derived in [21] and [22] which is effectively a SINR-based spectrum 'waterfilling' technique. This technique examines the interference spectrum and places the energy of the transmitted signal where the total interference is spectrally low. To execute this technique we start with the energy constraint for one transmit pulse of the radar transmitter which is given by

$$E_x = \int_{-W/2}^{W/2} |X(f)|^2 df \tag{2}$$

where $X(f)$ is the Fourier transform of the transmit waveform $x(t)$ and W is the effective bandwidth of the waveform. In other words, $|X(f)|^2$ maybe thought of as the ESD (energy spectral density) of the radar waveform. In the radar field, power (either peak or average) is usually used rather than energy. To accommodate for this we can let $|X(f)| = \sqrt{T}|S(f)|$) where T is clearly the duration of the transmit pulse and thus the waveform's PSD (power spectral density) is simply $|S(f)|^2 = |X(f)|^2/T$. The power can easily be calculated via $P_x = E_x/T$ or from the PSD via

$$P_x = \int_{-W/2}^{W/2} |S(f)|^2 df. \tag{3}$$

In practice when the radar return is received (after waveform transmission), clutter is picked up and also returned. If we let $h(t)$ be the clutter response then the clutter plus interference return (no target present) is given by

$$y(t) = x(t) * h(t) + q(t) + n(t). \tag{4}$$

Since the clutter $h(t)$ is usually random, we let $P_h(f)$ be the PSD of the clutter response which is present (for specific types of radar, e.g. ground-looking radar). In the frequency domain, the clutter plus interference PSD is given by

$$P_y(f) = |X(f)|^2 P_h(f) + P_q(f) + P_n(f) \tag{5}$$

where $P_q(f)$ and $P_n(f)$ are the PSDs of the communications interference and receiver noise respectively. We can simplify above by letting the interference plus noise PSD to be $P_i(f) = P_q(f) + P_n(f)$ and thus

$$P_y(f) = |X(f)|^2 P_h(f) + P_i(f). \tag{6}$$

The SINR may be maximized over the ESD term $|X(f)|^2$ given the energy constraint in (2). The complete SINR derivation and maximization may be performed via the Langragian multiplier technique and won't be shown here for brevity. The interested reader may look at the works in [21] and [22] and notice that these works may be extended to perform the derivation and optimization which result in a "waterfilling" solution.

The optimum ESD (i.e., the ESD resulting from SINR optimization) is "energy" filled via

$$|X(f)|^2 = \max\left(\frac{\sqrt{P_i(f)/\lambda} - P_i(f)}{P_h(f)},\ 0\right) \tag{7}$$

where λ (or $1/\lambda$) is a constant that needs to be calculated such that the above satisfies the energy constraint of the radar transmitter in (2). If we desire the power spectrum, we can divide $|X(f)|^2$ by T to arrive at the optimal PSD $|S(f)|^2$

and power can be calculated by $P_x = E_x/T$ or via (3). As with earlier works, we will continue to work with the radar waveform ESD $|X(f)|^2$.

B. BOUNDS FOR $1/\lambda$

It should be noted that (7) is only valid within certain conditions. First from the numerator of the non-zero term in (7) it can be seen that

$$\sqrt{P_i(f)/\lambda} > P_i(f) \tag{8}$$

for the output of (7) to remain above zero, otherwise (7) results in zero. Squaring both sides of (8) and dividing by $P_i(f)$ yield

$$1/\lambda > P_i(f) \tag{9}$$

which is a result noted in [22]. Since $P_i(f)$ is the PSD of interference plus noise, its minimum occurs at or above the noise only value of N_0 if we assume $P_n(f) = N_0$ (i.e., white noise PSD is constant). Therefore, the minimum value of $1/\lambda$ in order for the equation to have an output is N_0 which makes sense since it is the receiver (thermal) noise floor.

Now, the upper bound for $1/\lambda$ is more difficult to derive. For the result to be valid and to waterfill the spectrum due to $P_i(f)$, we look at the non-zero term of (7) as a function of $P_i(f)$. For ease of analysis let $A = 1/\lambda$. The non-zero part of the waterfilling equation becomes

$$\frac{\sqrt{AP_i(f)} - P_i(f)}{P_h(f)} \tag{10}$$

where the slope or derivative of (10) as a function of $P_i(f)$ can easily be derived. To this end the first derivative of the function with respect to $P_i(f)$ is given by

$$\frac{\sqrt{A}}{2P_h(f)\sqrt{P_i(f)}} - \frac{1}{P_h(f)}. \tag{11}$$

Given fixed values for A and $P_h(f)$, notice that as $P_i(f)$ approaches zero (from the right or positive values), the slope is mostly positive and approaches infinity as dictated by the square root of $P_i(f)$ in the denominator of the derivative. Since (7) needs to be applied in portions where its output values are decreasing, the variables $1/\lambda$ and $P_h(f)$ must be such that the first derivative remains negative throughout the range of $P_i(f)$. To insure this we set the first derivative less than zero, yielding

$$\frac{\sqrt{A}}{2P_h(f)\sqrt{P_i(f)}} < \frac{1}{P_h(f)} \tag{12}$$

which can be simplified to the result

$$\frac{A}{4} < P_i(f). \tag{13}$$

Substituting the original variables back into (13) indicates that (7) decreases with increasing $P_i(f)$ as long as

$$4 \min P_i(f) > \frac{1}{\lambda}. \tag{14}$$

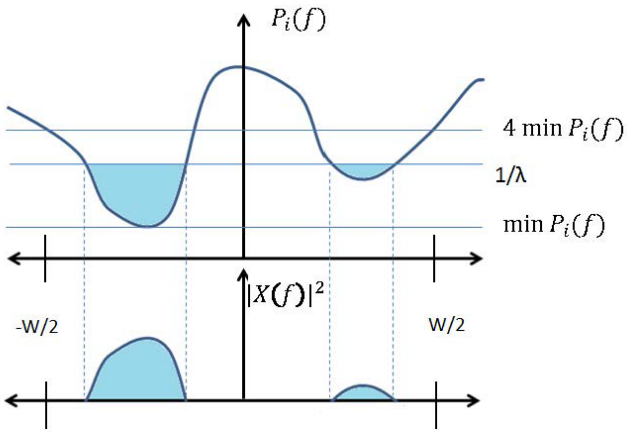

FIGURE 1. Illustration of the "waterfilling" or more appropriately "energyfilling" technique with proper bounds.

Therefore, the bounds of the waterfilling variable (which are critically important when the actual ESD spectrum is formed) are determined to be

$$\min P_i(f) < \frac{1}{\lambda} < 4 \min P_i(f). \tag{15}$$

We illustrate in Fig. 1 how waterfilling or more appropriately "energyfilling" is used to design $|X(f)|^2$ along with the maximum and minimum values of $1/\lambda$. From this illustration it is easy to see that nothing is energy-filled in $|X(f)|^2$ if $1/\lambda$ is chosen to be below $\min P_i(f)$. To actually find the value of $1/\lambda$ that ensures the optimum transmit spectrum $|X(f)|^2$ while making sure that the energy constraint is totally utilized (i.e. all energy is used for transmission), various algorithms may be used. For our simulations we utilize the well-known bisection algorithm. For brevity, the algorithm won't be discussed here. Interested reader may look at [31].

C. EFFECT OF NOT OBSERVING THE PROPER BOUNDS (SPECIALLY THE UPPER BOUND)

As mentioned, it is very important to observe the bounds when using the bisection algorithm to find $1/\lambda$ because false transmit waveform spectrum may result. To illustrate the erroneous effect of not following the upper bound, we illustrate in Fig. 2a a PSD for the legacy interference plus noise (where noise PSD is set to unity). In our example illustrated in Fig. 2a, we specifically allowed for the $1/\lambda$ to possibly take a value greater than $4 \min P_x(f)$. For convenience we set noise PSD to unity making the minimum value of $P_i(f)$ equal to 1. When the bound is violated, the output of the waterfilling procedure is flipped at some portions of the spectrum, i.e., the waterfilling action places more energy in the transmit spectrum at frequencies where there is considerable bandwidth utilization in the interference signal. Thus, if the resulting $1/\lambda$ is chosen or generated such that $1/\lambda > 4 \min P_x(f)$, then parts of the spectrum are filled incorrectly, and the radar places considerable amount of its energy in the middle of the communications spectrum which can cause negative results for both systems (i.e. each

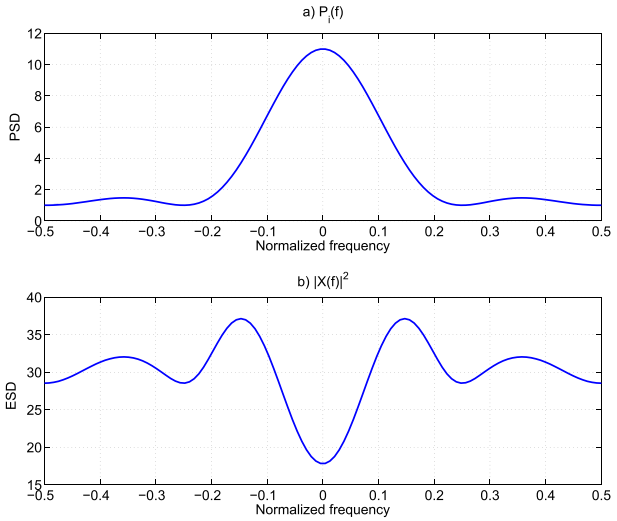

FIGURE 2. An example of a "waterfilled" or energy-filled output when $1/\lambda$ limits are not observed when trying to find the proper value of $1/\lambda$ (that ensures the optimum waveform spectrum is found) using any search algorithm such as a bisection algorithm: a) the QPSK spectrum (plus noise) in which the mainlobe bandwidth is about half the spectrum available for the radar signal and b) the resulting "erroneous" radar energy spectrum.

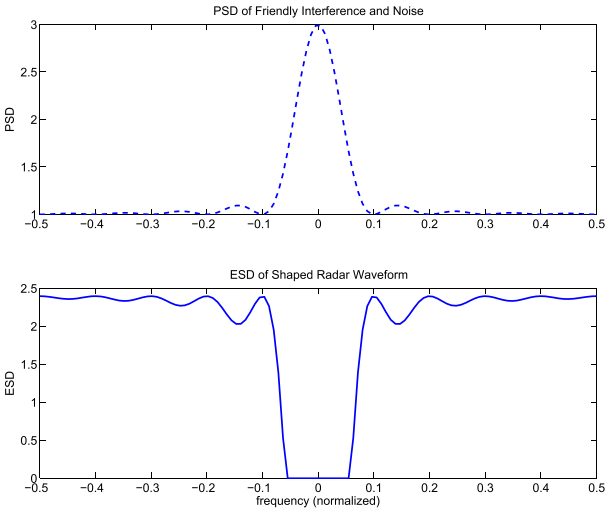

FIGURE 3. Top Panel: PSD of a communication system employing QPSK modulation (plus noise) with a small mainlobe bandwidth compared to the total spectrum available to the radar signal. Bottom Panel: ESD of resulting radar transmit signal.

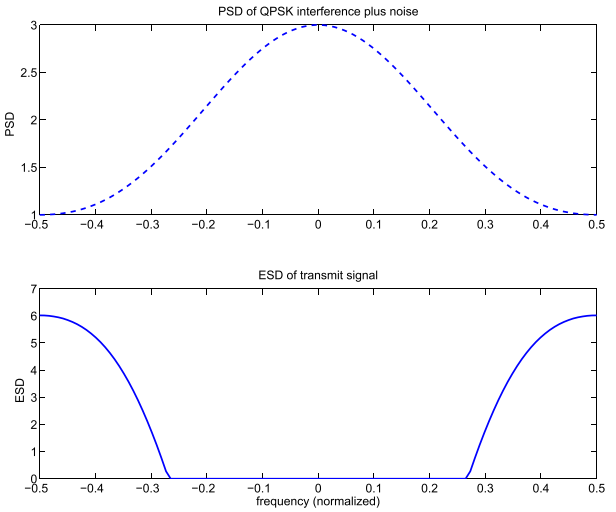

FIGURE 4. Top Panel: PSD of a communication system employing QPSK modulation (plus noise) with a mainlobe bandwidth equal to the total spectrum available to the radar signal. Bottom Panel: ESD of resulting radar transmit signal.

interferes with the other). The resulting radar waveform spectrum for this example is shown in Fig. 2b. Notice that while the transmit spectrum allocated some amount of power in the communication system mainlobe, it does not directly avoid it as intuition would suggest. Clearly, the transmit spectrum is non-optimal and is a non-desirable result of not carefully selecting the bounds when using a search-based optimization algorithm such as the bisection technique.

D. SPECTRALLY SHAPED RADAR WAVEFORM EXAMPLE FOR COMMUNICATION SYSTEM EMPLOYING QPSK

In this section we properly show (by observing the proper bounds) how a radar waveform spectrum is spectrally shaped (to be 'friendly') while considering the spectrum of a legacy communication system (which acts as 'not-so-friendly' interference since it affects the radar's detection performance). Consider two legacy communication systems whose sinc-type spectra are shown in the top panel of Fig. 3 and 4. In both Fig. 3 and 4, the thermal noise PSD is again set to unity such that the nulls of the sinc-type spectra have values of 1. In this work, various modulations and their corresponding spectra can be easily accommodated. For the results reported in this paper, it is enough to choose one modulation for illustration and to generate various scenarios and simulation results. We will use quaternary phase-shift keying (QPSK) modulation. We will not pursue to add traditional pulse shaping in to the QPSK symbols (since that is not the focus of this paper) although it should be fairly straightforward to incorporate it into the communication PSDs. In Fig. 3, the mainlobe of the QPSK spectrum is much smaller than the available or total spectrum. In Fig. 4, the mainlobe of the QPSK signal actually occupies the entire spectrum. It will be interesting to illustrate how radar waveform spectra are formed for these two different QPSK plus noise spectra (i.e., one may be thought as narrowband while the other may be thought of as wideband). Via (7), we can calculate the optimum radar transmit spectra. The resulting optimal spectra of the radar pulse are shown in the bottom panel of Fig. 3 and 4. In Fig. 3 notice how the transmit spectrum avoided most of the mainlobe of the QPSK plus noise PSD. The resulting waveform spectrum fills the rest of the total available spectrum in a very special way. Notice that the resulting spectrum is not flat. Instead, the waterfilling procedure places more energy in the nulls of the communication bandwidth to take advantage of those nulls. As for the time-domain waveform, since the spectrum of the waveform somewhat resembles that of a notched filter, the time-domain waveform

would look like that of a notched filter impulse response. We elect to show the spectrum of the radar waveform since it clearly shows how the communication band is avoided by the spectrally-shaped radar waveform for shared access and spectrum management purposes.

For the case in Fig. 4 it is clear that the radar has no choice but to place energy somewhere in the available spectrum and thus would interfere with the legacy signal. What's interesting however is that the waterfilling procedure placed most of the energy at the edges of the legacy's signal mainlobe by taking advantage of those 'low' interference areas while minimizing the effect to the communication system's center frequencies. Clearly there could be plenty of time-domain waveforms that fit the spectrum since the optimal spectrum is phase tolerant [20], [21]. For the simulations in this work, it is sufficient to chose one realization of the many possible ones. Furthermore, we see the difference in the two transmit spectra based on both the legacy spectra and amount of spectrum available to the radar.

III. DETECTION PERFORMANCE FOR THE SHAPED RADAR WAVEFORM AND SER OF THE COMMUNICATION SYSTEM

A. RECEIVER PROCESSING AND PERFORMANCE APPROXIMATION

Now given a realization of the transmit waveform we form the two detection hypotheses given by

$$\mathcal{H}_0 : x(t) = s(t) * h(t) + q(t) + n(t) \tag{16}$$

$$\mathcal{H}_1 : x(t) = As(t) + s(t) * h(t) + q(t) + n(t) \tag{17}$$

where $x(t)$ is the received signal, $s(t)$ is the transmit signal, $As(t)$ is the deterministic radar response of a point target, $h(t)$ is the clutter response, the convolution $s(t) * h(t)$ is the clutter echo, $q(t)$ is the QPSK random communication signal, and $n(t)$ is AWGN noise. $\mathcal{H}_0$ represents the return when no target is present and $\mathcal{H}_1$ represents the return when a point target is present. The term A can be random to accommodate fluctuating targets where the work in [22] can be used. But in our application, we are clearly more interested in the effect of communication interference rather than fluctuating targets or signal-dependent clutter. Thus, we assume unit amplitude for target simulation purposes i.e. $A = 1$ and we assume that $h(t)$ to be small (compared to legacy interference plus noise) in (16)-(17). Moreover, we conveniently transition to discrete-time signal model. Of course, we assume proper time sampling as dictated by the Nyquist sampling theorem. For convenience, we assume unit time instant $T_s = 1$. Then the discrete time detection hypotheses are

$$\mathcal{H}_0 : \mathbf{x} = \mathbf{q} + \mathbf{n} \tag{18}$$

$$\mathcal{H}_1 : \mathbf{x} = \mathbf{s} + \mathbf{q} + \mathbf{n}. \tag{19}$$

If the radar receiver is simply under thermal (Gaussian) noise, then the receiver filter is simply the filter matched to the target-waveform echo. Unfortunately, the radar is also interfered with the communication signal. The optimum detector should incorporate the fact that the QPSK interference is random (i.e. four phases) and the proper probability distribution due to this type of interference. Moreover, the proper distribution may also be a function of the relative received timing between the radar pulse and random interference symbol. In other words, the optimum detector is very difficult to derive due to the addition of non-Gaussian interference to additive white Gaussian noise of the receiver. In this work, we propose a suboptimal detector. Note that even though our friendly QPSK interference is not Gaussian, it is nonetheless a random signal whose autocorrelation function can easily be calculated. We temporarily assume that the total interference to be Gaussian such that we can use the generalized matched filter detector for correlated Gaussian noise. We use this as our sub-optimum detector in this work. For the purposes of generating interim performance curves (via theoretical calculations), we can calculate the detection performance since we have the correlation matrix of the QPSK signal $\mathbf{C}_q$ given by the matrix with the primary diagonal equal to σ_q^2 and each successive diagonal decreasing by $\frac{1}{N}\sigma_q^2$ where N is the number of radar samples in a single QPSK symbol. Thus, the interference correlation matrix is given in the equation as shown at the bottom of this page.

We let $\mathbf{C}$ be the correlation matrix of interference plus noise. Since the correlation matrix of AWGN noise is $\mathbf{C}_n = \sigma_n^2 I$, then the correlation matrix is given by

$$\mathbf{C} = \mathbf{C}_n + \mathbf{C}_q. \tag{20}$$

However, to produce more accurate performance curves we perform Monte Carlo simulations and compare these to the approximate theoretical results. We start by looking at the *pdf* under each of the two hypotheses assuming the total interference to be correlated Gaussian process given by

$$p(\mathbf{x}|\mathcal{H}_0) = \frac{1}{\pi^N \det(\mathbf{C})} \exp[-\mathbf{x}^H \mathbf{C}^{-1} \mathbf{x}] \tag{21}$$

$$p(\mathbf{x}|\mathcal{H}_1) = \frac{1}{\pi^N \det(\mathbf{C})} \exp[-(\mathbf{x}-\mathbf{s})^H \mathbf{C}^{-1} (\mathbf{x}-\mathbf{s})] \tag{22}$$

$$\mathbf{C_q} = \begin{bmatrix} \sigma_q^2 & \sigma_q^2(1-\frac{1}{N}) & \dots & \sigma_q^2(1-\frac{N-1}{N}) & 0 \\ \sigma_q^2(1-\frac{1}{N}) & \sigma_q^2 & \dots & \dots & \sigma_q^2(1-\frac{N-1}{N}) \\ \dots & \dots & \dots & \dots & \dots \\ 0 & \sigma_q^2(1-\frac{N-1}{N}) & \dots & \sigma_q^2(1-\frac{1}{N}) & \sigma_q^2 \end{bmatrix}$$

where we decide $\mathcal{H}_1$ if a certain threshold (γ) is met, i.e. that a target is present if

$$\frac{p(\mathbf{x}|\mathcal{H}_1)}{p(\mathbf{x}|\mathcal{H}_0)} > \gamma \tag{23}$$

which is easily reduced to

$$\mathrm{Re}[-\tilde{s}^H \mathbf{C}^{-1}\mathbf{x}] > \gamma' \tag{24}$$

where γ' is the modified threshold. It can be shown that the theoretical probability of detection P_d and probability of false alarm P_{FA} are given by

$$P_d = Q\left(\frac{\gamma' - s^H \mathbf{C}^{-1} s}{\sqrt{\frac{s^H \mathbf{C}^{-1} s}{2}}}\right) \tag{25}$$

$$P_{FA} = Q\left(\frac{\gamma'}{\sqrt{\frac{s^H \mathbf{C}^{-1} s}{2}}}\right) \tag{26}$$

where $Q(\cdot)$ stands for the Q-function. Solving equation (26) for γ' yields

$$\gamma' = \sqrt{\frac{s^H \mathbf{C}^{-1} s}{2}} Q^{-1}(P_{FA}) \tag{27}$$

and substituting (27) back into equation (25) yeilds

$$P_d = Q\left(Q^{-1}(P_{FA}) - \sqrt{d^2}\right) \tag{28}$$

where the deflection coefficient is given by

$$d^2 = 2\mathbf{s}^H \mathbf{C}^{-1} s. \tag{29}$$

We note that even though we assume clutter to be small (compared to interference plus noise), we do not necessarily set it to zero in our simulations to keep our scenarios realistic.

B. DETECTION PERFORMANCE OF SHAPED RADAR WAVEFORM VIA MONTE CARLO SIMULATION AND COMPARISON TO APPROXIMATE THEORETICAL EXPRESSION

In this section, we formulate an example scenario where the radar forms the waveform as dictated in (7) while considering a communication signal whose PSD is very much like the PSD shown in Fig. 3 and report the probability of detection performance P_d. Recall we consider a communication signal employing QPSK modulation. We can use the approximate theoretical expression in (28) for P_d for the radar receiver. We recall that since we are considering the radar receiver, SIR pertains to radar return being the signal and the communication signal being the interference. This is very important. Later on when we consider the communication system, SIR would actually mean signal being the QPSK signal and interference would actually mean the radar signal. Going back to reporting detection performance, we show in Fig. 5 the detection curves for the radar based on (28) indicated by the dashed lines (as opposed to the solid and dotted lines) given three values of P_{FA} as a function of SIR in dB. In this particular example, the interference-to-noise ratio (INR) is set

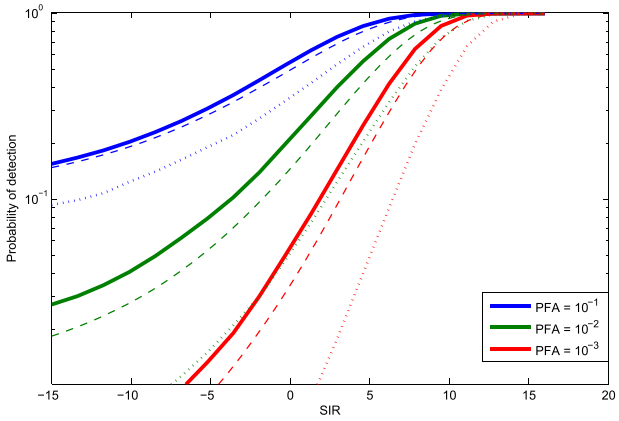

FIGURE 5. Probability of detection vs SIR (in dB) for each selected probability of false alarm: a) dashed lines are performance curves from theoretically calculated result based of (28), b) solid lines are the performance results from Monte Carlo simulation when the shaped spectrum pulse is used, and c) the dotted lines are performance results using a traditional wideband pulsed waveform.

at 3 dB. Recall that (28) is only a theoretical approximation due to the fact that we assumed the total interference to be Gaussian. To account for the fact that the total interference is the sum of non-Gaussian QPSK random symbols and Gaussian receiver noise, we perform extensive Monte Carlo experiments to produce more accurate detection curves indicated by solid lines in Fig. 5. The two sets of detection curves are close, albeit the approximate theoretical curves are clearly pessimistic results compared to the actual Monte Carlo results. It should now be clear that the performance differences are attributed to the fact that the equations assumed correlated Gaussian interference in calculating the detection threshold (γ') when in fact our QPSK interference is a random information signal. During Monte Carlo simulations, γ' was adjusted manually until the decided P_{FA} was attained.

Finally the detection performance of the spectrally-shaped transmit waveform can be compared to the detection performance of a traditional wideband pulse radar with communication interference present. Recall that the goal of the shaped transmit waveform is to mitigate the effect of the interference (again QPSK signal in this case). Performance curves in Fig. 5 not only illustrates the actual performance of the shaped waveform is better than the theoretically approximated equation (28) but also shows a marked improvement in detection performance over that of traditional wideband pulse radar. For a selected P_{FA} of 0.01 and a SIR of 3 dB we get an improvement in the probability of detection from 0.12 to 0.40 which shows a 3 to 1 improvement in detection.

C. EFFECT ON P_{cs} AND SER OF A COMMUNICATIONS SYSTEM

Another objective of the shaped transmit waveform design is to minimize the disruptive effect to the legacy communication systems. In the case of a system employing QPSK modulation, our goal is to minimize the effect on probability of correct symbol detection P_{cs}. In communication

systems the complement of P_{cs} is the SER which is more commonly reported (i.e., $SER = 1 - P_{cs}$). The idea is to not make any system changes (software or hardware) to the legacy communication system, i.e. the communication system is unaware of the radar's beneficial waveform design. In other words, the legacy system is effectively unharmed and radar disruption is reduced. This means the communication receiver uses its original matched filter detector for QPSK without any additional signal processing or hardware upgrade. With the use of shaped transmit radar waveform, the result is the mitigation of effect on P_{cs} performance. While we will later concentrate on reporting SERs (since SER is the metric more commonly used by communication engineers) it is very instructive to quickly look at P_{cs} curve as a function increasing radar-to-QPSK signal ratio or interference-to-signal ratio (ISR). In other words, we should actually observe P_{cs} to suffer as ISR is increased.

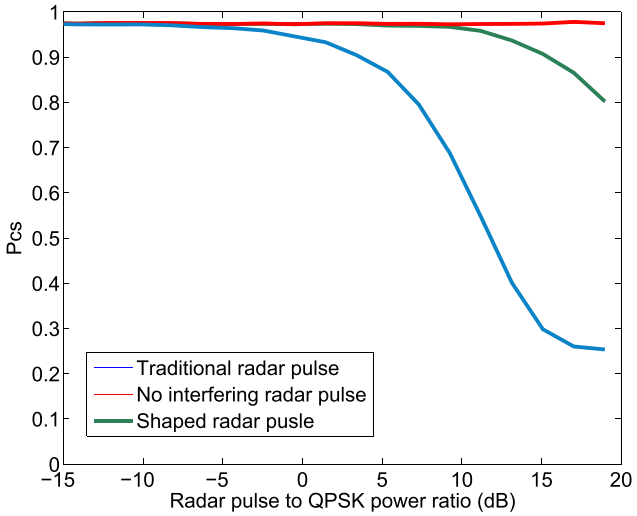

FIGURE 6. Probability of correctly detecting a QPSK symbol P_{cs} vs. ISR in dB when: traditional wideband radar pulse is present as an interferer (labeled 'Traditional radar pulse'); no interference (labeled 'No interfering radar pulse); and when the shaped radar pulse is used (labeled 'Shaped radar pulse').

In Fig. 6 we show the P_{cs} of a legacy QPSK system. The redline indicates the P_{cs} performance of the system when no radar signal present (no interference), i.e., this is the performance of the legacy system under thermal noise. Since thermal noise is also ever present, here we have selected a SNR of 3 dB (i.e., QPSK signal to AWGN noise ratio). Using a theoretical expression, this would amount to 0.9542 but since the P_{cs} shown is actually a result of Monte Carlo simulations, the P_{cs} curve varies by a very small amount as would be expected from Monte Carlo simulations. We then introduce a traditional wideband radar pulse. Via Monte Carlo simulations, we calculate the probability (actually percentage) of detecting the correct symbol with radar-to-QPSK power ratios ranging from -15 dB to $+20$ dB. From the Fig. 6, we can see from resulting P_{cs} curve (labeled 'Traditional radar pulse') that the wideband radar pulse has

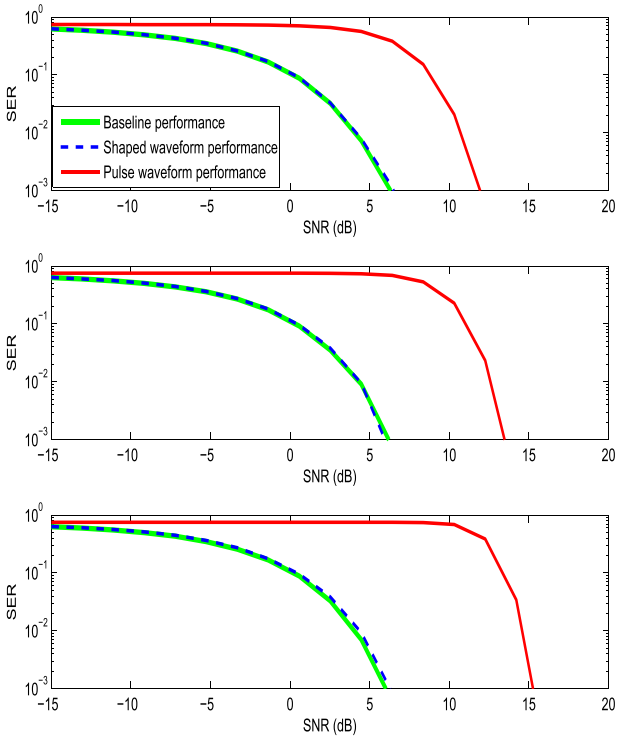

FIGURE 7. SER vs. SNR curves for QPSK receiver. Top panel: 3 dB radar to noise ratio or INR. Middle panel: 6 dB radar to noise ratio or INR. Bottom panel: 9 dB radar to noise power ratio or INR.

a disruptive effect on the communication system starting at about the -4 dB ISR. We then show the performance of the un-altered QPSK detector when the shaped transmit waveform is used. Here we see that this waveform does not begin to interfere with the communications detector until the 10 dB radar-to-QPSK power ratio is reached (see curve labeled 'Shaped radar pulse'). This is a marked improvement of the communications detector's ability to correctly demodulate the communication signal compared to when the traditional radar pulse is used. In other words, this improvement comes from no adjustments to the legacy communication system but is simply a realized side effect of our use of the spectrally-shaped radar pulse.

We now switch to the more common communication performance metric: SER. An effective way to assess SER is to parameterize the radar power to noise power ratio or simply INR and present the SER vs SNR curves. In Fig. 7, we show the SER vs. SNR (in dB) performance curves of a QPSK receiver when a radar signal is the interference. Here we can compare the SER performances when the shaped radar pulse is present and when traditional radar pulse is present. To measure the effectiveness of the shaped transmit waveform in minimizing its effect on the communication systems, we also plot the SER for the scenario where there is only white noise i.e. no radar present labeled as 'Baseline performance' which is also produced by Monte Carlo simulations (which we have verified to match the theoretical performance). For the top panel of Fig. 7,

the radar to noise ratio or INR is 3 dB. In the middle panel it is 6 dB and finally the INR is 9 dB in the bottom panel. QPSK baseline performance without a radar signal present is provided in each panel for comparison. As can be seen from Fig. 7, the communication receiver works very well as if no radar transmit signal is present with even a 9 dB INR ratio provided the radar is using the spectrally shaped radar pulse. In contrast, the communication receiver's performance is severely limited even with only a 3 dB INR when a traditional wideband pulse is used.

IV. RADAR P_d AND RADIO SER WITH A SINGLE COMMUNICATION SYSTEM

In this section we consider the detection performance effect of a single-user communication system on a radar using the shaped radar waveform. Of course, we also consider the converse, i.e., the SER performance effect of that radar signal on a single communication system. We consider two variations depending on the bandwidth of the communication signal compared to the available spectrum.

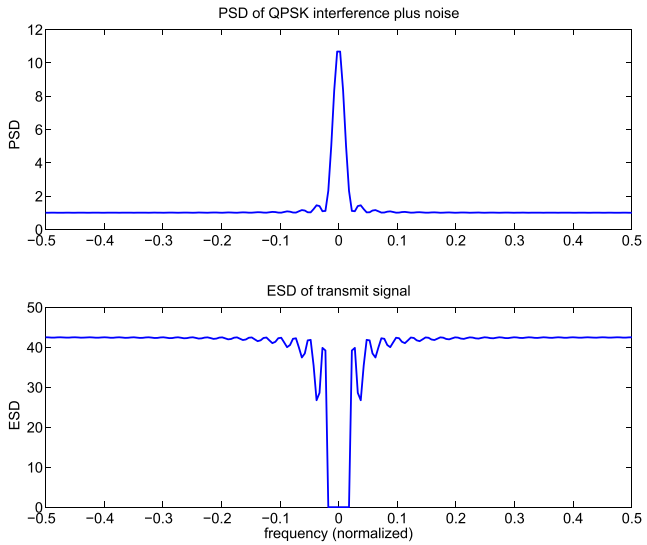

FIGURE 8. Top panel: PSD of QPSK (plus noise) with mainlobe bandwidth that is $(1/20)^{th}$ of the available spectrum. Bottom panel: ESD of resulting radar transmit signal.

A. SINGLE COMMUNICATION SYSTEM WITH NARROW BANDWIDTH

The first communication system considered is a narrowband signal whose mainlobe is $1/20^{th}$ times the available spectrum. The spectrum of the QPSK interferer is shown in Fig. 8 (top panel). In Fig. 8 (bottom panel) the ESD of the shaped radar waveform (using an energy constraint $E_s = 40$) is shown. Notice that over 95 percent of the energy of the waveform is placed outside the mainlobe of the communications signal. It is interesting to note that the radar waveform spectrum resembles that of the spectrum a 'notched' filter. Intuitively, this situation allows the two systems to perform almost as if the other signal is not present as seen from the performance curves in Fig. 9 and Fig. 10.

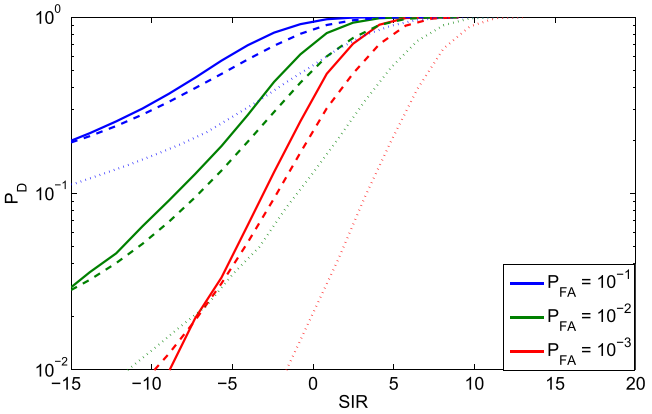

FIGURE 9. Probability of detection versus SIR in dB (for each selected probability of false alarm) for a radar system where there is a single communication system whose bandwidth is much less than that of the available spectrum for the radar: a) dashed lines are performance curves from theoretically calculated result based of (28), b) solid lines are the performance results from Monte Carlo simulation when the shaped spectrum pulse is used, and c) the dotted lines are performance results using a traditional wideband pulsed waveform.

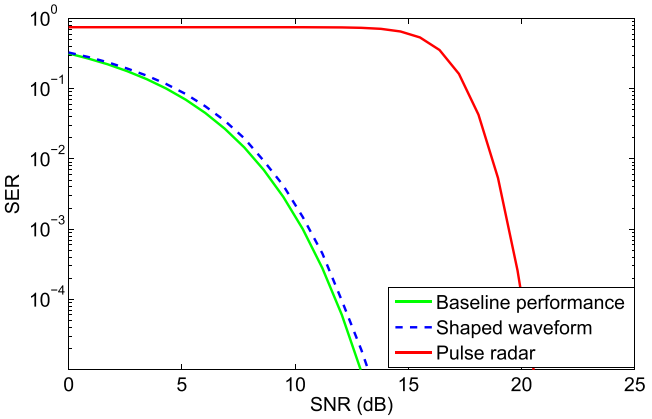

FIGURE 10. SER performance curves for QPSK receiver with 9 dB radar-to-noise ratio for a single narrowband communication system.

In Fig. 9 the detection performance of the radar as a function of increasing SIR (here the radar signal is increased while the QPSK power is held constant). In this scenario, we set the QPSK interference to noise ratio (or INR) is 10 dB. With a PFA of 10^{-3}, the performance of the radar with a 3 dB SIR improves from a P_d of 0.09 (with the use of traditional wideband pulsed waveform) to 0.78 (using the shaped radar waveform). This is a marked improvement over the traditional radar pulse signal.

In Fig. 10 the SER vs. SNR performance curves of the QPSK receiver are depicted for this scenario where the radar signal to noise ratio (or INR) is 9 dB. With the use of traditional pulse radar signal, the communication receiver's SER performance is so degraded (compared to the theoretical expression of QPSK SER where no interference is present) that it does not start getting better until 15 dB of SNR is used. Indeed it does not start improving until the QPSK signal to radar power ratio is at least 6 dB. The performance curve

for the legacy communication system with the shaped radar signal present very closely follows the theoretical expression of QPSK SER where no interference is present. This result indicates that the communication system works as if no radar is present even during the radar transmit time.

It should be noted that the clutter PSD $P_h(f)$ may also play an important role in deciding the shape of the spectrum. In Fig. 11 we see what happens when $P_h(f)$ is decreased, causing (7) to fill the spectrum quicker and, consequently, be more sensitive to the lower values of $P_h(f)$. This is because of the signal-dependent nature of the clutter interference. In fact, the shaped waveform takes great advantage of deep clutter nulls. In reality, we do not have control over $P_h(f)$ but it is clear that a waveform can be formed regardless.

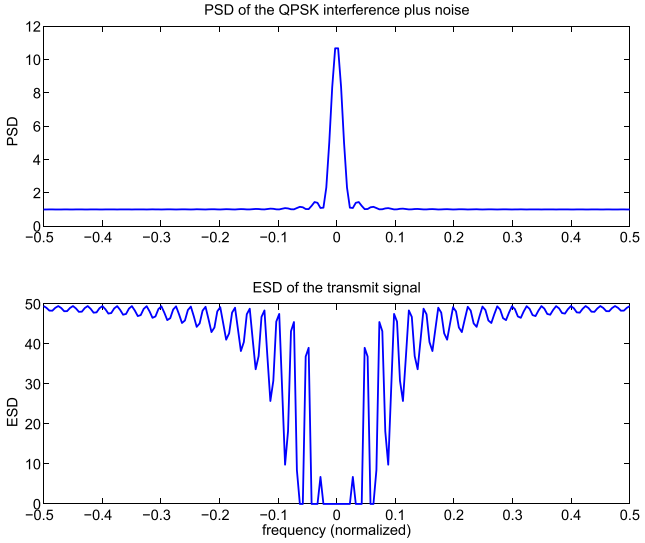

FIGURE 11. Top panel: the same QPSK spectrum used in Fig. 8. Bottom panel: the resulting ESD with lower values of $P_h(f)$.

B. SINGLE COMMUNICATION SYSTEM WITH WIDE BANDWIDTH

In this scenario, we consider the case when the communication mainlobe bandwidth is equal to the available spectrum, i.e., the communication mainlobe completely spans the spectrum available to the radar. This case is applicable to wideband communication systems in which the bandwidths may be comparable to radar bandwidths.

In Fig. 12 (top panel) the mainlobe of the communication PSD (plus noise) is shown. Clearly, the radar does not have a choice but to place the energy in the mainlobe of the communication signal if it were to form the spectrally-shaped radar waveform. Interestingly, however, the waveform created still keeps the energy out of the very center of the main lobe as seen in Fig. 12 (bottom panel). In Fig. 13 it is clear that shaped waveform radar's detection performance as a function of SIR in dB (where we recall that SIR is clearly radar-to-QPSK power ratio) is superior to that of the traditional pulse's performance. In this special case where the communication mainlobe spans the full available spectrum

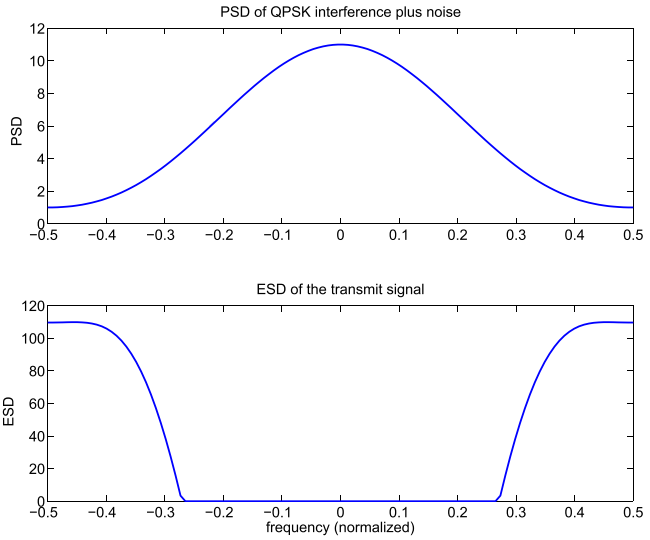

FIGURE 12. Top panel: PSD of a QPSK signal in which the mainlobe spans the available spectrum. Bottom panel: ESD of the resulting radar transmit signal.

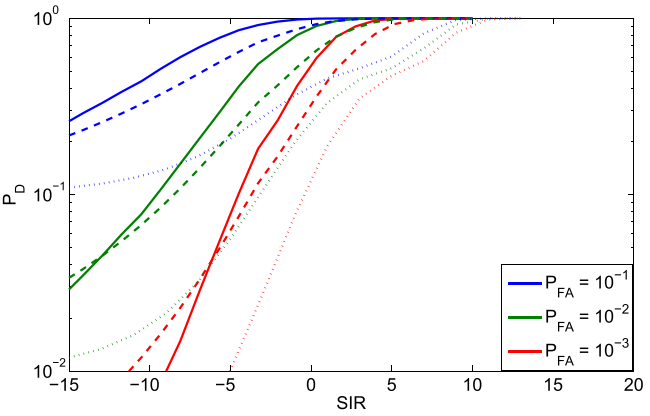

FIGURE 13. Probability of detection versus SIR in dB (for each selected probability of false alarm) for a radar system with one communication system interferer whose bandwidth is equal to that of the available spectrum: a) dashed lines are performance curves from theoretically calculated result based of (28), b) solid lines are the performance results from Monte Carlo simulation when the shaped spectrum pulse is used, and c) the dotted lines are performance results using a traditional wideband pulsed waveform.

it can be observed that when the radar energy or power constraint is small relative to the interfering communication signal, it has a distinct spectral shape that focuses the radar's energy away from the center of the communication signal frequency. But as the radar signal power grows, the radar actually starts to spill energy over to the communication signal's mainlobe.

In Fig. 14 we show the SER performances of the communication receiver when the shaped radar waveform is present and when the traditional pulsed waveform is present. With the use of traditional pulse radar signal, the communication receiver's SER performance is severely degraded (compared to the theoretical expression for QPSK SER where no interference is present). With the use of the shaped

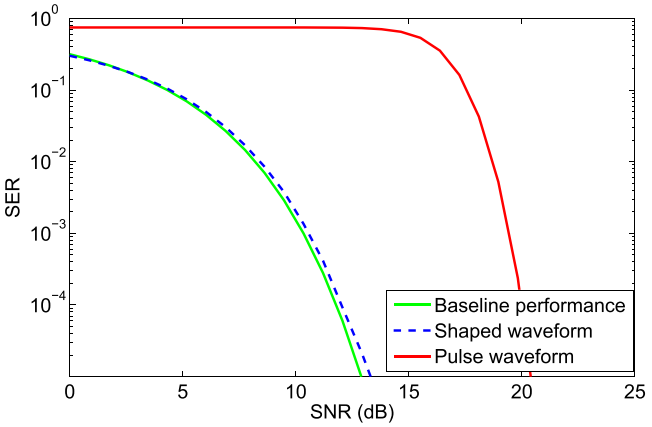

FIGURE 14. SER performance curves for QPSK receiver with 9 dB radar-to-noise ratio for a single wideband communication system.

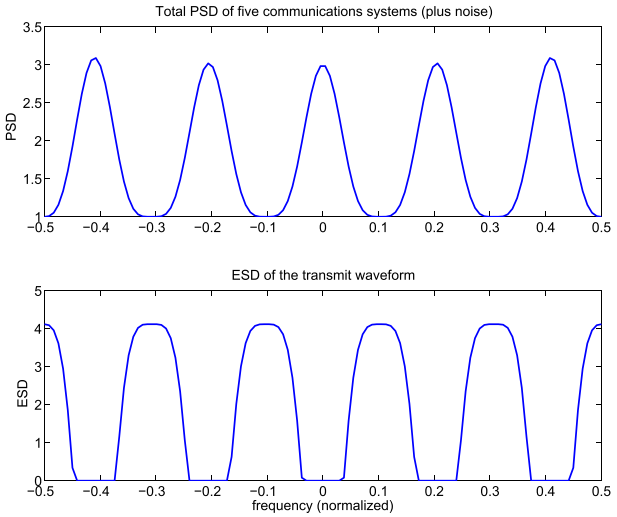

FIGURE 15. Top Panel: PSD of multiple (5) QPSK signals each with bandwidth of 1/5 of the spectrum available to the radar signal. Bottom panel: ESD of the resulting radar transmit signal.

radar waveform, we can see the communication signal is not appreciably interfered with since the radar placed its energy away from the center frequency of the communication signal.

V. RADAR P_d AND RADIO SER WITH MULTIPLE COMMUNICATION SYSTEMS

A. FIVE COMMUNICATION SYSTEMS: EACH WITH BANDWIDTH THAT IS 1/5 OF TOTAL AVAILABLE SPECTRUM

We now look at the case when multiple communication signals are present in the portion of the spectrum available to the radar. In the top panel of Fig. 15 we see that there are five sinc-type main lobes corresponding to five PSDs in the portion of the spectrum available to the radar. In the bottom panel we see the shaped radar pulse spectrum. We note that the radar places its energy in the frequencies between these communication signals and avoids the center of each main lobe of the communication signals entirely. It is interesting to

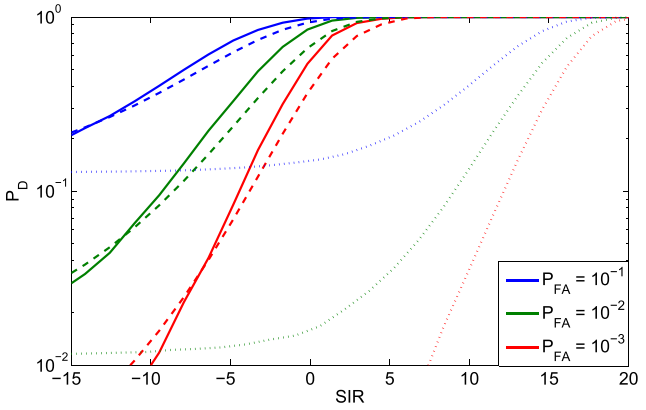

FIGURE 16. Probability of detection versus SIR in dB (for each selected probability of false alarm) for a radar system with multiple legacy QPSK interferers where the mainlobe bandwidth of each interferer is 1/5 of total spectrum: a) dashed lines are performance curves from theoretically calculated result based of (28), b) solid lines are the performance results from Monte Carlo simulation when the shaped spectrum pulse is used, and c) the dotted lines are performance results using a traditional wideband pulsed waveform.

note that the radar waveform spectrum resembles that of the spectrum a 'comb-shaped' filter.

In Fig. 16 we can see the radar detection performance with the theoretical approximation, with the wideband pulse, and shaped radar waveform. Notice that there is a dramatic increase in P_d corresponding to the shaped waveform over the traditional pulse waverform. Except for the very low SIR region, the P_d performance of the shaped radar waveform is better than the approximation provided by (28).

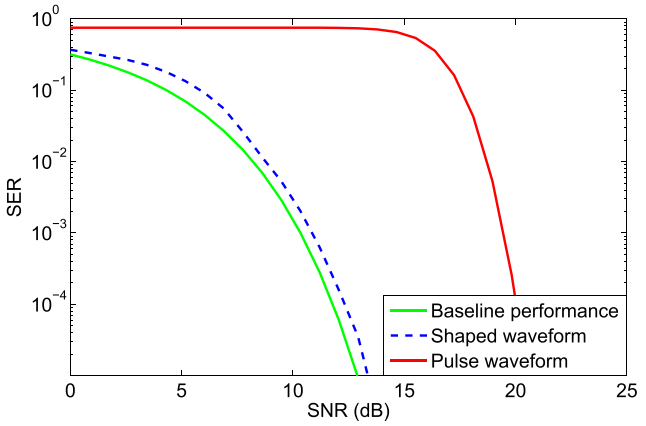

FIGURE 17. SER performance curve for a QPSK receiver with 9 dB radar-to-noise ratio (one sample SER from the five communication systems).

For brevity, we report the the SER performances of only one of the five communication receivers without radar interference (labeled 'Baseline performance'), with the shaped radar waveform (labeled 'Shaped waveform'), and with the wideband pulsed waveform (labeled 'Pulse waveform') in Fig. 17. One set of SER results is sufficient since the SER results are very similar. Here we notice that the SER performance of one of the communication systems is

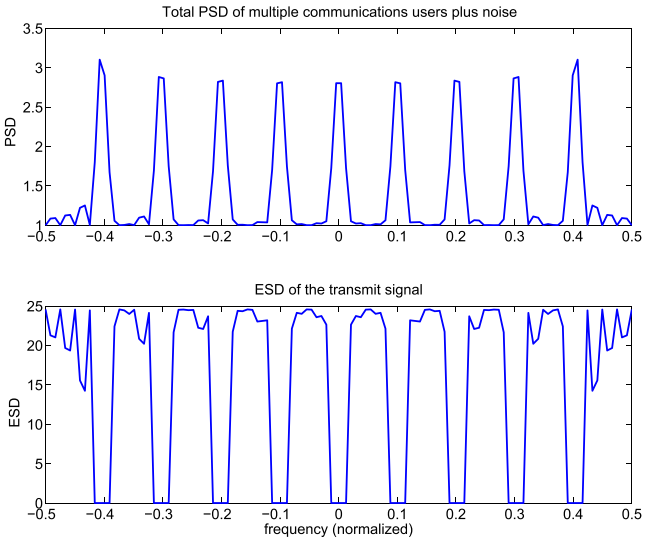

FIGURE 18. Top panel: PSD of multiple (9) QPSK signals with each mainlobe bandwidth of 1/20th of the available spectrum. Bottom panel: ESD of resulting radar transmit signal.

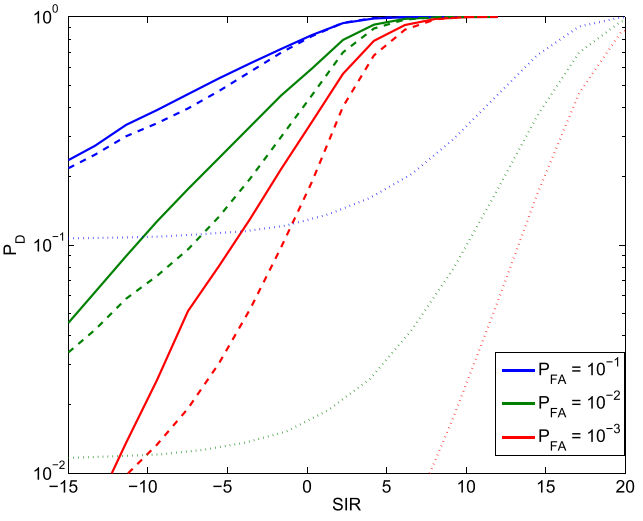

FIGURE 19. Probability of detection versus SIR in dB (for each selected probability of false alarm) for a radar system with multiple 'friendly' QPSK interferers where the mainlobe bandwidth of each interferer is 1/20 of total spectrum: a) dashed lines are performance curves from theoretically calculated result based of (28), b) solid lines are the performance results from Monte Carlo simulation when the shaped spectrum pulse is used, and c) the dotted lines are performance results using a traditional wideband pulsed waveform.

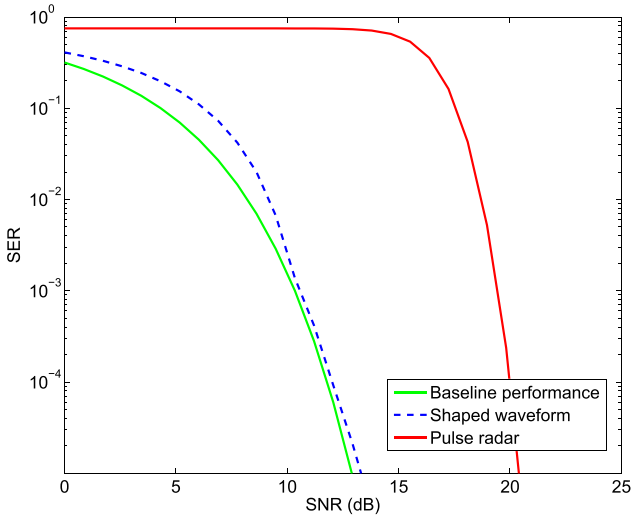

FIGURE 20. SER performance curve for a QPSK receiver with 9 dB radar-to-noise ratio (one sample SER from the nine communication systems).

still close to the QPSK SER theoretical performance. Moreover, it again shows a marked improvement over the case when the pulsed radar signal is present.

B. NINE COMMUNICATION SYSTEMS: EACH WITH BANDWIDTH THAT IS 1/20 OF TOTAL AVAILABLE SPECTRUM

In this scenario, the available spectrum is 20 times that of the mainlobe bandwidth of a single communication system. This is similar to the case in Section IV.A (Single communication system with narrow bandwidth) except we now consider nine communications signals present in the available spectrum (as shown in top panel of Fig. 18). With so many communication systems, it would be interesting to see the resulting ESD for the shaped radar pulse. In Fig. 18 (bottom panel) it can be seen that the radar places its energy in the gaps between the communications signals. Intuitively, the radar employing the shaped radar waveform tries to minimally interfere with all of the nine communication systems as a way to share access and manage the spectrum. Conversely, the nine communication systems minimally interfere with the radar receiver (and none of them even know they're doing it!). It is evident in Fig. 19 that the detection performance curves for the wideband pulsed radar (shown here with dotted lines) suffer dramatically. In terms of spectrum sharing, it is evident in this scenario (from Fig. 18) that the radar employing the shaped waveform clearly maximizes the use of the remaining spectrum while minimizing the interference effect on the other nine communication bands.

Again for brevity only one of the nine communication signals is checked for SER in Fig. 20 and the SER performance curve presented is for that one system. Notice that more radar waveform energy is now in the main lobe of each communications system (compared to a single communication system scenario). This effect makes the performance of a communication system suffer slightly at lower signal-to-noise ratios compared to the scenario dictated in Section IV.A where there is only one communication user where the SER is shown in Fig. 14.

VI. INCORPORATING THE RADAR DUTY CYCLE TO SER PERFORMANCE

Continuous wave (CW) radars transmit for a considerable amount of time (at least compared to pulsed radar systems) and thus can wipe out communication systems during

TABLE 1. Conditional SER of the QPSK receiver for the given scenarios.

SNR	No radar present	Pulsed radar	Single narrowband comms with shaped radar waveform	Multiple (nine) narrowband comms with shaped radar waveform	Multiple (five) wideband comms with shaped radar waveform	Single wideband comms with shaped radar waveform
6 dB	0.046	0.75	0.057	0.11	0.093	0.050
9 dB	0.0051	0.75	0.0071	0.014	0.0088	0.0064
12 dB	0.00007	0.74	0.00012	0.00012	0.00019	0.00012

TABLE 2. Effective SER of the QPSK receiver for the given scenarios.

SNR	No radar present	Pulsed radar	Single narrowband comms with shaped radar waveform	Multiple (nine) narrowband comms with shaped radar waveform	Multiple (five) wideband comms with shaped radar waveform	Single wideband comms with shaped radar waveform
6 dB	0.046	0.053	0.046	0.047	0.046	0.046
9 dB	0.0051	0.013	0.0051	0.0052	0.0051	0.0051
12 dB	0.00007	0.0075	0.000071	0.000071	0.000071	0.000071

transmit time and the SERs reported in Sections IV-V apply. However, pulsed radar systems such as pulsed-Doppler systems operate on a duty cycle. In other words (for pulsed radar systems), the wipeouts (or dropouts) are conditioned during the pulse time. If we let d_c be the duty cycle of the radar, SER_c be the conditional SER, and SER_N be the SER due to thermal noise only, then effective SER_E can be calculated via

$$\text{SER}_E = (1 - d_c)(\text{SER}_N) + d_c(\text{SER}_c). \tag{30}$$

To compare the conditional SER_c and the effective SER_E, we summarize the SER_c of the four scenarios in Sections IV-V in Table 1 for SNRs equal to 6, 9, and 12 dB. Recall that these are the SERs during the actual transmit portion of the radar signal. Duty cycles are driven by practical specifications. For illustration purposes, let's consider an example where radar has a duty cycle of 0.01. With this information we can now calculate the total SER_E for the communications receiver using 0.01 as the duty cycle for a communication receiver (take one sample system from the multiple communication scenario). The effective SERs are presented in Table 2.

The effective SER (SER_E) is obviously better than the conditional SER (SER_c). Of course, this is true for a communication receiver under the wideband pulsed interference as well. For example, with a 9 dB SNR the SER_c is 0.75 and SER_E is 0.013. While this is a good improvement, an SER of 0.013 does not meet practical SER specifications. Of course, we already know that the SER_c for a communication receiver under the shaped radar waveform interference is close to the theoretical SER. As such, the corresponding SER_E is also better. These results suggest that the radar employing spectrally-shaped waveform can coexist with the communication system and not have appreciable impact on that system while maintaining its own detection performance.

VII. SUMMARY

In this paper we investigated a 'friendly spectrally-shaped' radar waveform design technique that can be used in a channel being utilized by one or more legacy communication systems. The idea was to design a waveform that is able to share the spectrum with the communication systems such that its detection performance is not compromised while trying to help the communication systems maintain their own SERs. We considered the very important case where existing legacy communications are unaltered (i.e., they are static in the frequency domain and do not have the inherent capability to share the spectrum) since legacy technologies have a tendency to linger. The result was a radar pulse waveform that was able to utilize what remains of the available spectrum (for both shared access and spectrum management) such that the SNR or SINR is maximized which resulted in 'waterfilling' or 'energy-filling' waveforms. We showed using various examples and scenarios where the shaped radar waveform outperforms the traditional wideband pulse waveform (in communication interference) in terms of detection performance. In these examples, we used QPSK as example modulation. Moreover, SERs of the legacy communication systems with shaped radar waveform (acting as interference) outperform SERs of legacy systems resulting with traditional radar pulse (acting as interference). In fact, these SERs are very close to theoretical SERs (noise-only).

REFERENCES

[1] R. D. Campbell, "Radar interference to microwave communication services," *Trans. Amer. Inst. Elect. Eng., I, Commun. Electron.*, vol. 77, no. 5, pp. 717–722, Nov. 1958.
[2] K. Shepherd, private communication, Sep. 2012.
[3] President's Council of Advisors on Science and Technology, "Report to the president: Realizing the full potential of government-held spectrum to spur economic growth," Executive Office President, Washington, DC, USA, Tech. Rep., Jul. 2012.

[4] The National Science Foundation. *Enhancing Access to the Radio Spectrum (EARS)*. [Online]. Available: http://www.nsf.gov/pubs/2015/nsf15550/nsf15550.pdf, accessed Jul. 2015.
[5] Strategic Technology Office and Defense Advanced Research Projects Agency. *Shared Spectrum Access for Radar and Communications (SSPARC)*. [Online]. Available: http://www.darpa.mil/program/shared-spectrum-access-for-radar-and-communicationss, accessed Jul. 2015.
[6] L. S. Wang, J. P. McGeehan, C. Williams, and A. Doufexi, "Application of cooperative sensing in radar–communications coexistence," *IET Commun.*, vol. 2, no. 6, pp. 856–868, Jul. 2008.
[7] R. Saruthirathanaworakun, J. M. Peha, and L. M. Correia, "Opportunistic sharing between rotating radar and cellular," *IEEE J. Sel. Areas Commun.*, vol. 30, no. 10, pp. 1900–1910, Nov. 2012.
[8] J. T. Johnson, C. J. Baker, H. Wang, L. Ye, and C. Zhang, "Assessing the potential for spectrum sharing between communications and radar systems in the L-band portion of the RF spectrum allocated to radar," in *Proc. IEEE Int. Conf. Electromagn. Adv. Appl. (ICEAA)*, Aug. 2014, pp. 331–334.
[9] L. Wang, J. McGeehan, C. Williams, and A. Doufexi, "Radar spectrum opportunities for cognitive communications transmission," in *Proc. 3rd Int. Conf Cognit. Radio Oriented Wireless Netw. Commun.*, May 2008, pp. 1–6.
[10] C. de Souza Lima, F. Paisana, J. Ferreira de Rezende, and L. A. DaSilva, "A cooperative approach for dynamic spectrum access in radar bands," in *Proc. Int. Telecommun. Symp. (ITS)*, Aug. 2014, pp. 1–5.
[11] C. Sturm, T. Zwick, and W. Wiesbeck, "An OFDM system concept for joint radar and communications operations," in *Proc. IEEE 69th Veh. Technol. Conf.*, Apr. 2009, pp. 1–5.
[12] S. Sen and A. Nehorai, "Adaptive design of OFDM radar signal with improved wideband ambiguity function," *IEEE Trans. Signal Process.*, vol. 58, no. 2, pp. 928–933, Feb. 2010.
[13] G. Lellouch, P. Tran, R. Pribic, and P. van Genderen, "OFDM waveforms for frequency agility and opportunities for Doppler processing in radar," in *Proc. IEEE Radar Conf. (RADAR)*, May 2008, pp. 1–6.
[14] M. Bica and V. Koivunen, "Frequency agile generalized multicarrier radar," in *Proc. 48th Annu. Conf. Inf. Sci. Syst. (CISS)*, Mar. 2014, pp. 1–6.
[15] The Department of Defense. (2013). *Electromagnetic Spectrum Strategy: A Call to Action*. [Online]. Available: http://www.defense.gov/news/dodspectrumstrategy.pdf
[16] Various Agencies. (2012). *Joint Electromagnetic Spectrum Management Operations*. [Online]. Available: http://www.dtic.mil/doctrine/new_pubs/jp6_01.pdf
[17] B. van Niekerk and C. Cloete, "Management information systems for electronic warfare command and decision support," *J. Inf. Warfare*, vol. 14, no. 1, Apr. 2015.
[18] K.-W. Huang, M. Bica, U. Mitra, and V. Koivunen, "Radar waveform design in spectrum sharing environment: Coexistence and cognition," in *Proc. IEEE Radar Conf.*, Arlington, VA, USA, May 2015, pp. 1698–1703.
[19] M. R. Bell, N. Devroye, D. Erricolo, T. Koduri, S. Rao, and D. Tuninetti, "Results on spectrum sharing between a radar and a communications system," in *Proc. Int. Conf. Electromagn. Adv. Appl. (ICEAA)*, Aug. 2014, pp. 826–829.
[20] M. R. Bell, "Information theory and radar waveform design," *IEEE Trans. Inf. Theory*, vol. 39, no. 5, pp. 1578–1597, Sep. 1993.
[21] R. A. Romero, J. Bae, and N. A. Goodman, "Theory and application of SNR and mutual information matched illumination waveforms," *IEEE Trans. Aerosp. Electron. Syst.*, vol. 47, no. 2, pp. 912–927, Apr. 2011.
[22] S. Kay, "Optimal signal design for detection of Gaussian point targets in stationary Gaussian clutter/reverberation," *IEEE J. Sel. Topics Signal Process.*, vol. 1, no. 1, pp. 31–41, Jun. 2007.
[23] K. D. Shepherd and R. A. Romero, "Radar waveform design in active communications channel," in *Proc. IEEE Asilomar Conf. Signals, Syst., Comput.*, Pacific Grove, CA, USA, Nov. 2013, pp. 1515–1519.
[24] D. Erricolo, H. Griffiths, L. Teng, M. C. Wicks, and L. Lo Monte, "On the spectrum sharing between radar and communication systems," in *Proc. Int. Conf. Electromagn. Adv. Appl. (ICEAA)*, Aug. 2014, pp. 890–893.
[25] H. He, P. Stoica, and J. Li, "Waveform design with stopband and correlation constraints for cognitive radar," in *Proc. 2nd Int. Workshop Cognit. Inf. Process. (CIP)*, Elba, Italy, Jun. 2010, pp. 344–349.
[26] A. Aubry, A. De Maio, M. Piezzo, and A. Farina, "Radar waveform design in a spectrally crowded environment via nonconvex quadratic optimization," *IEEE Trans. Aerosp. Electron. Syst.*, vol. 50, no. 2, pp. 1138–1152, Apr. 2014.
[27] A. Aubry, A. De Maio, Y. Huang, M. Piezzo, and A. Farina, "A new radar waveform design algorithm with improved feasibility for spectral coexistence," *IEEE Trans. Aerosp. Electron. Syst.*, vol. 51, no. 2, pp. 1029–1038, Apr. 2015.
[28] S. D. Blunt, P. Yatham, and J. Stiles, "Intrapulse radar-embedded communications," *IEEE Trans. Aerosp. Electron. Syst.*, vol. 46, no. 3, pp. 1185–1200, Jul. 2010.
[29] J. G. Metcalf, C. Sahin, S. D. Blunt, and M. Rangaswamy, "Analysis of symbol design strategies for intrapulse radar-embedded communications," *IEEE Trans. Aerosp. Electron. Syst.*, to be published.
[30] W.-Q. Wang, "Large time-bandwidth product MIMO radar waveform design based on chirp rate diversity," *IEEE Sensors J.*, vol. 15, no. 2, pp. 1027–1034, Feb. 2015.
[31] T. K. Moon and W. Stirling, *Mathematical Methods and Algorithms for Signal Processing*. Englewood Cliffs, NJ, USA: Prentice-Hall, 1999.

RIC A. ROMERO (S'07–M'10–SM'12) received the B.S.E.E. degree from Purdue University, in 1999, the M.S.E.E. degree from the University of Southern California, in 2004, and the Ph.D. degree in electrical and computer engineering from the University of Arizona, in 2010.

He was a Senior Multidisciplined Engineer II with Raytheon Missile Systems, Tucson, AZ, from 1999 to 2010. He was involved in various communications, radar, and research and development programs. He was also a Graduate Research Assistant with the Laboratory for Sensor and Array Processing, University of Arizona, from 2007 to 2010. He is currently an Assistant Professor with the Department of Electrical and Computer Engineering, Naval Postgraduate School, Monterey, CA. His research interests are in the general areas of radar, sensor information processing, and communications.

Dr. Romero received the 2004 Corporate Excellence in Technology Award and a Company-Wide Technical Prize at Raytheon Corporation. He also received the Raytheon Advanced Scholarship Program Fellowship from 2002 to 2004 and 2005 to 2007.

KEVIN D. SHEPHERD received the B.S. degree from the University of Kansas, in 2002, and the master's degree in electrical engineering from Naval Postgraduate School, in 2013. He was a Marine Pilot and a Major at U.S. Marine Corps. He is currently a U.S. Marine Corps Officer.